Pronounced nonlinear behavior of atomic collision sequences induced by keV-energy heavy ions in solids and molecules

V. I. Shulga,* M. Vicanek,† and P. Sigmund
Fysisk Institut, Odense Universitet, DK-5230 Odense M, Denmark
(Received 27 July 1988)

When an energetic ion hits a target consisting of atoms lighter than the projectile, the target configuration seen by the ion along its trajectory may differ significantly from the initial state. This nonlinear effect, which originates in rapidly moving recoil atoms, has been investigated by molecular-dynamics simulation mainly for the simple case where the target is a diatomic molecule. Nonlinear behavior has been distinguished from linear behavior by, respectively, switching on and off the interaction between target particles. Pronounced nonlinear effects have been found in energy loss and scattering angle of the ion; they have been classified roughly as clearing-the-way and blocking-the-way effects, depending on whether nonlinear behavior results in a low or high scattering probability. Effects on stopping power appear small for the small systems investigated. For ion-molecule collisions, the important conclusion is made that binary-scattering behavior need not be indicative of a spectator collision but may, if the ion mass exceeds the target mass, originate in the (nonlinear) clearing-the-way effect. The paper ends with a few results and tentative conclusions on ion-surface scattering with heavy ions.

I. INTRODUCTION

The conventional picture of multiple scattering processes undergone by heavy ions in matter is similar to that valid for electrons, neutrons, protons, and other light particles interacting with a material medium; it is strictly a linear one. It assumes that changes in the target, caused by the bombarding particle, do not have a noticeable feedback effect on the motion of that particle. The assumption appears justified if the pertinent changes in the structure and/or state of motion of the medium are either weak or rare or too much delayed to affect the motion of the projectile. An exception which is characteristic of the long range of the Coulomb interaction is the screening effect on the projectile charge by the electrons of the penetrated medium.

In the present work we wish to explore specific nonlinearities caused by *fast atoms recoiling from collisions with heavy ions.* The basic idea is as follows.[1] Consider (Fig. 1) an ion 1 (energy E, mass M_1) colliding with a target atom 2 (mass M_2) at rest. The ion may transfer a substantial fraction of its energy to the atom, and if $M_1 > M_2$, the speed of the latter may be higher than the final or even the initial projectile speed. Therefore, the recoil atom may run ahead of the projectile and clear the way for the latter. Here, the term "clearing the way" is suggestive of removing obstacles along the path of the projectile, but the opposite effect, piling up obstacles, cannot be excluded from the outset. In Fig. 1 atom 4 will be kicked away from the ion trajectory. The key point is that, unlike in the case of light penetrating particles, the projectile itself need not be the leading disturbance at any point of the trajectory. Hence, the frequency distribution of scattering processes undergone by the ion is affected by earlier collision events on the same trajectory. In view of this lack of linear superposition of the effects due to individual ion-atom collisions, we talk about nonlinear behavior.

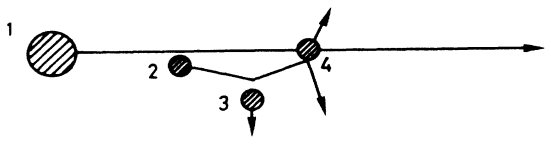

FIG. 1. Target atoms recoiling from collisions with heavy penetrating ion 1 may change the structure and state of motion of the medium in front of the ion. From Ref. 1.

Processes involving recoil atoms are significant if the cross section for elastic collisions is sizeable, i.e., for heavy ions and target atoms at energies in the eV- or keV-energy range. The process sketched above, hinging on the relative speeds of the incident ion and recoil atom, is expected to show up if the ion mass M_1 is noticeably larger than the target mass M_2, and to increase with increasing mass difference. Measurable effects might be expected in ion-solid, in particular ion-surface, and ion-molecule or ion-cluster collisions.

Peculiarities in atomic collision cascades initiated by heavy ions have previously been pointed out in terms of displacement spikes,[2] collision spikes,[3] or shock waves.[4] None of these concepts takes into account the above-mentioned clearing-the-way function played by fast recoil atoms. The feature is ignored not only in conventional linear collision cascade theory,[5] but also in Monte Carlo[6] or binary collision[7] simulation codes that either totally ignore or do not fully incorporate the real-time sequence of collision events. The effect is evidently also ignored in a

simple scaling law relating energy loss and scattering angle in ion-molecule collisions.[8]

II. COMPUTATIONAL MODEL

Figure 1 indicates that the detailed behavior in time and space of the particle trajectories may affect the sign and magnitude of the nonlinear features to be investigated; hence, a molecular-dynamics investigation appears appropriate for an initial exploration. Limitations in computer capacity confine conventional simulations of this kind—which attempt to simulate complete collision cascades—to quite low primary energies;[9] in the present situation, however, we need to simulate only very small sequences of collision events to show the effect, and hence, computer capacity does by no means set an upper limit on projectile energy. For the purpose of pinpointing nonlinear behavior, the main requirements are a substantial cross section for elastic collisions and the feasibility of experimental verification. In the keV-energy range, both requirements are well satisfied.

At energies above a few keV, details of the interatomic potential must be of minor importance for the qualitative nature of the interaction processes. In particular, pertinent recoil energies are large enough to let the *repulsive* ion-atom and atom-atom interactions dominate at the rather small impact parameters of interest. Thus, attractive interactions will be taken as unimportant and ignored even when we deal with *ion-molecule* collisions.

Also the quantal character of atomic collisions will be neglected: Even though it will turn out that small changes in impact parameter ($\cong 0.01$ Å) may lead to dramatic changes in scattering angle, typical de Broglie wavelengths for the collisions to be analyzed are of the order of 10^{-4} Å. Hence, classical mechanics governs the trajectories of the collision partners.

The computer program used here was rewritten on the basis of a well-established molecular dynamics code[10] utilizing an average-force algorithm.[11] It simulates copper target atoms bombarded by noble-gas ions, mostly xenon. Target atoms have been arranged as diatomic or polyatomic molecules at interatomic distances pertinent to crystalline solids or gaseous molecules, and the (binary) interaction potential was, for simplicity, chosen as[10]

$$V(R)=\begin{cases} C/R^2, & R<2a \\ C(e/2a)^2\exp(-R/a), & R>2a \end{cases} \quad (1)$$

where $C=3.05Z_1Z_2(Z_1^{1/2}+Z_2^{1/2})^{-2/3}$ eV Å^2, $a=0.196$ Å, $e=2.718$, and R is the internuclear distance. This potential has been obtained by matching (in value and slope) a Born-Mayer potential with the screening radius a from Ref. 12 to an R^{-2} potential with the constant C governed by the screening radius of Ref. 13. With this potential, for Xe on Cu, ion-target and target-target interactions are Born-Mayer-like up to $E\cong 10$ keV. Ion-target and target-target interaction potentials are cut off at a distance of 4.0 Å. Integrations are performed with the time step chosen such that the change in energy during any step does not exceed 0.1% for any particle. Under these conditions, computation times on our local Apollo network are typically a few seconds per collision event if all pertinent data are to be displayed on the screen, and much less otherwise.

The elementary event to be analyzed is an ion-diatom collision. In order to distinguish nonlinear from linear events, all collision sequences have been simulated in two distinctly different ways.

Model 1: In a linear model, only ion-target interactions are taken into account while the target-target interaction potential is set equal to zero. Evidently, perturbations in the target can only be caused by the ion itself in this model.

Model 2: In a model allowing for nonlinear effects, both ion-target and target-target interactions are taken into account. Evidently, clearing the way (or blocking it) by recoil atoms is possible in this model.

Computations were stopped whenever all interacting particles had moved apart from each other to distances greater than the cutoff radius of the interaction potential, i.e., 4 Å. We note that strong nonlinear effects are expected mainly for small impact parameters, i.e., close collisions (Fig. 1).

III. COMPARISON OF LINEAR WITH NONLINEAR BEHAVIOR

Figure 2(a) shows the energy E of a xenon projectile with initial energy $E_0=5$ keV after colliding with a copper dimer oriented parallel to the initial velocity as a function of impact parameter p. The internuclear distance of the dimer was chosen as 3.61 Å, corresponding to the cube length in a Cu crystal. It is seen that models 1 and 2 yield identical results for $p>0.15$ Å which, as a matter of fact, reflect the binary (ion-atom) scattering law shown by the dotted line. Drastically different energies are found at lower impact parameters. For $0.1\text{ Å}\le p\le 0.15$ Å, model 2 predicts a lower energy—or higher energy loss—while the opposite is true for $p\le 0.1$ Å.

Figure 2(b) shows the corresponding behavior of the scattering angle θ of the projectile. Roughly, model 2 predicts a larger scattering angle in the range of impact parameters where also the energy loss is larger, and vice versa, yet the crossover points differ slightly.

Figures 2(a) and 2(b) show that for $p<0.1$ Å and almost down to zero the collision follows accurately the binary ion-atom scattering law in case of model 2, i.e., atom 2 has been knocked off the trajectory. This is by no means the case in model 1. Thus, these graphs present strong evidence in favor of the predicted clearing-the-way effect.

Figure 3 shows particle trajectories for representative impact parameters. The dots and numbers indicate time: Equal numbers on different trajectories indicate equal times. However, the time scale is not linear but has been chosen to yield constant path-length increments on the ion trajectory.

Figures 3(a) and 3(b) demonstrate the point just made: In model 1, the ion interacts violently with atom 2 [Fig. 3(a)] while in model 2 [Fig. 3(b)], atom 2 has been

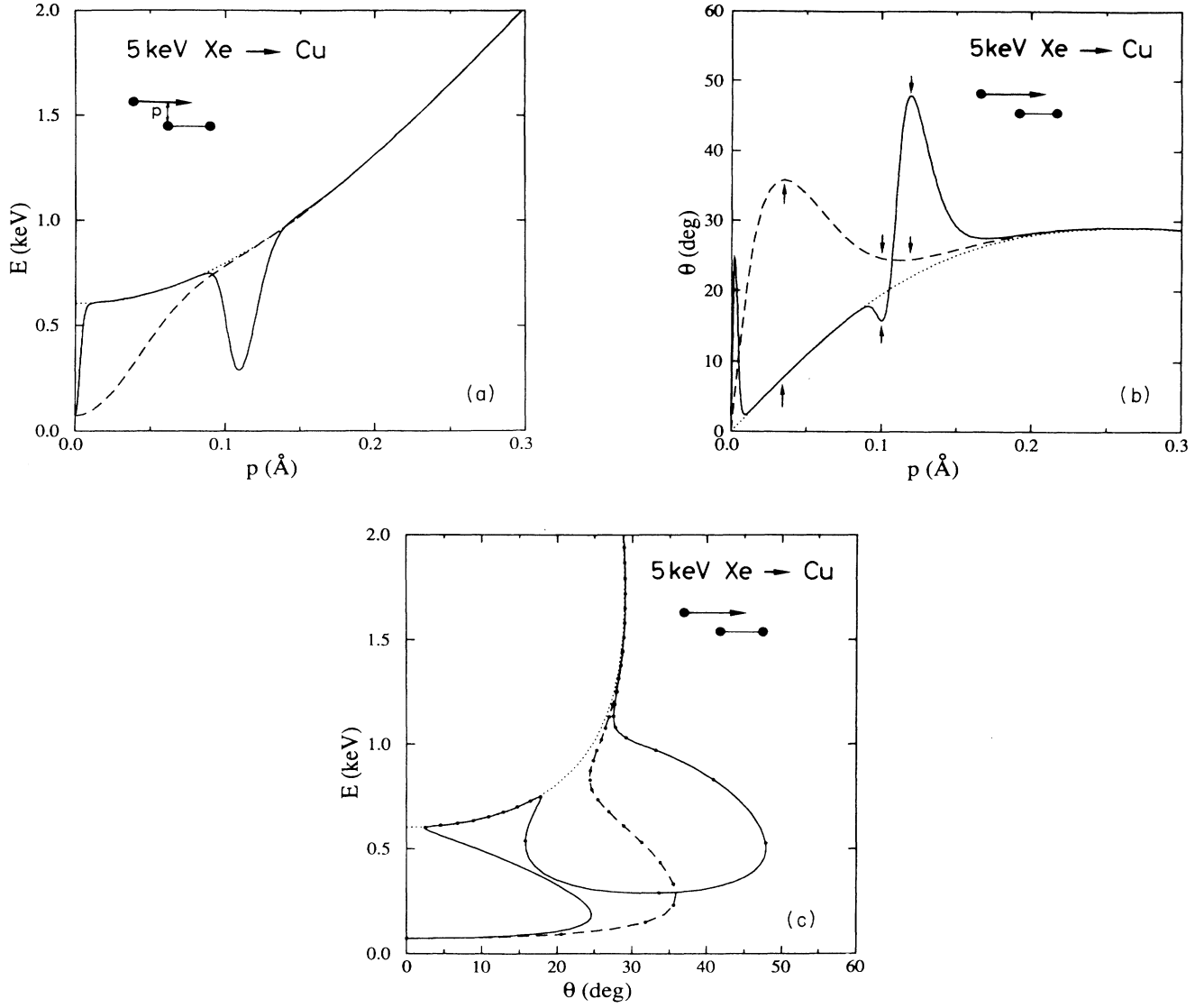

FIG. 2. Scattering of 5-keV Xe by a Cu dimer. Internuclear distance $d = 3.61$ Å corresponding to cube length in copper crystal. Dashed line: model 1, target-target interaction ignored. Solid line: model 2, target-target interaction included. Dotted line: binary ion-atom collision only. (a) Projectile energy E after collision vs impact parameter p. (b) Total scattering angle of projectile θ vs impact parameter p. Arrows indicate impact parameters for which trajectories are shown in Fig. 3. (c) E vs θ, found from (a) and (b) by eliminating p. Dots reflect equidistant impact parameters.

knocked off by atom 1 a long time before arrival of the ion. Similar features are found in Figs. 3(c) and 3(d) for $p = 0.10$ Å, although the interaction with atom 2 is very weak even for model 1 [Fig. 3(c)]. However, for $p = 0.12$ Å, the relation is reversed, and atom 1 kicks atom 2 into the trajectory of the ion just at the right time to cause a violent interaction [Fig. 3(f)] that would not be expected from the linear model [Fig. 3(e)]. This results in a pronounced dip in the energy [Fig. 2(a)] and a peak in the scattering angle [Fig. 2(b)]. Thus, Figs. 2(a) and 2(b) also contain convincing evidence in support of a blocking-the-way effect.

Note that there is only a small variation in the scattering angles from the interaction with atom 1 when the impact parameter varies from $p = 0.10$–0.12 Å; therefore, model 1 makes very similar predictions for the outcome of the double scattering events in the two cases. Conversely, model 2 yields a violent interaction with atom 2 for $p = 0.12$ Å and almost none for $p = 0.10$ Å, despite very similar trajectories in space. The reason for the difference is the different timing, as indicated in the graphs.

Figure 2(c) combines Figs. 2(a) and 2(b), the impact parameter being eliminated but still indicated as dots on an E versus θ plot. Neighboring dots correspond to equidistant impact parameters. Note that E is a (single- or

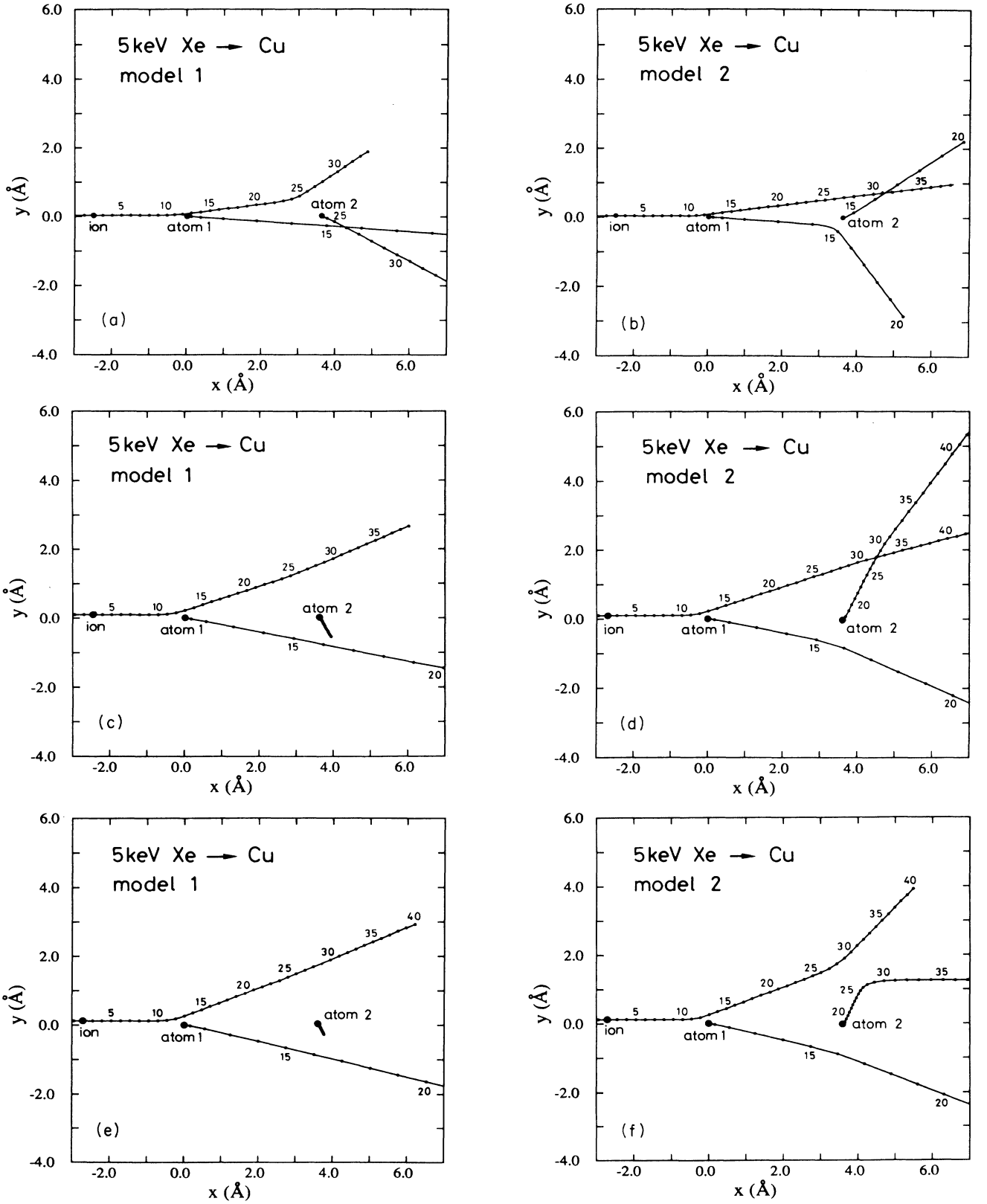

FIG. 3. Trajectories corresponding to collision specified in Fig. 2 for three distinct impact parameters. Planar motion. Dots and numbers symbolize time. The time interval is chosen to yield equal path-length increments *on the ion trajectory*. (a) $p = 0.035$ Å. Model 1. (b) $p = 0.035$ Å. Model 2. (c) $p = 0.10$ Å. Model 1. (d) $p = 0.10$ Å. Model 2. (e) $p = 0.12$ Å. Model. 1. (f) $p = 0.12$ Å. Model 2.

multiple-valued) function of θ only for a fixed orientation of the target relative to the projectile velocity. For a randomly oriented target molecule, the energy is continuously distributed as discussed below.

A low density of dots in Fig. 2(c) is equivalent to a small cross section. Lines have been included here to guide the eye but will be left out as far as possible in further graphs of this type in order to give a more balanced impression of the relative importance of the different branches in the E versus θ plot.

Figures 4(a) and 4(b) demonstrate that the nonlinear behavior is also found for krypton bombardment, but over a narrower range of impact parameters, while the opposite trend is seen for uranium ions. Thus, our initial expectation is confirmed of an effect to be found mainly for $M_1 > M_2$ and increasing with increasing mass difference.

Figures 5(a) and 5(b) indicate that the magnitude of the difference in relative energy loss found from models 1 and 2, respectively, is rather insensitive to the initial energy E_0, but that the range of pertinent impact parameters increases with decreasing energy. We have also found little sensitivity to the interatomic distance except for scaling with the impact parameter.

Figure 6 shows that the effect is not quite insensitive to the interatomic potential: Of the four potentials utilized, the pure R^{-2} potential differs noticeably from all the others by a long tail which tends to smear the separability of individual ion-atom collisions, regardless of whether they are linear or nonlinear. Consequently, it exhibits a very different scattering behavior. Disregarding this extreme case, we still find a noticeable variation in the pertinent

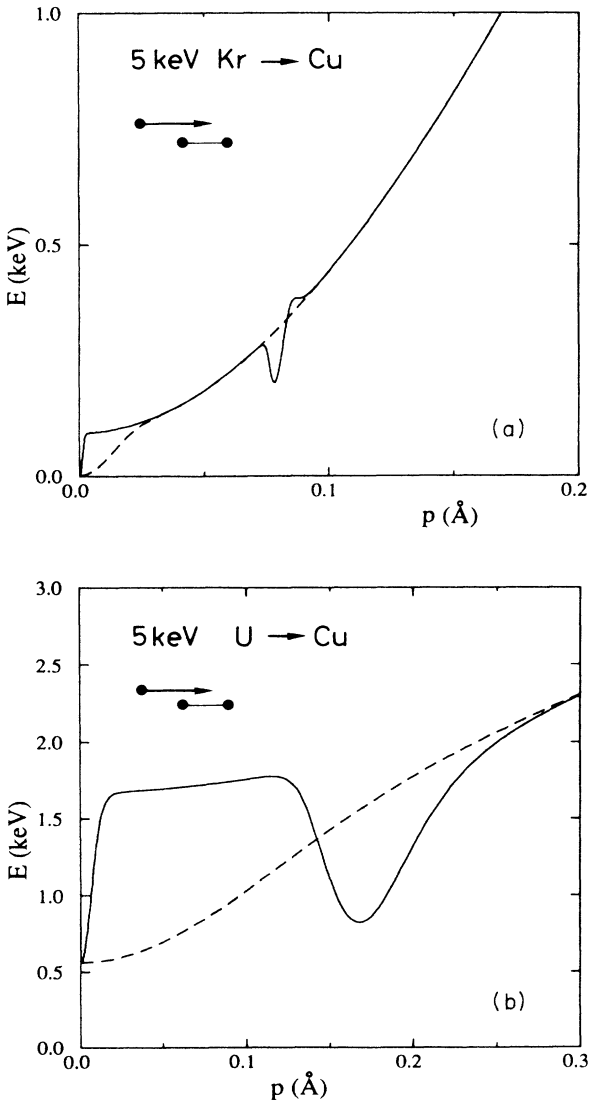

FIG. 4. Same as Fig. 2 with Xe replaced by lighter or heavier ion. Dashed line: model 1. Solid line: model 2. (a) Krypton ion. Energy vs impact parameter. (b) Uranium ion. Energy vs impact parameter.

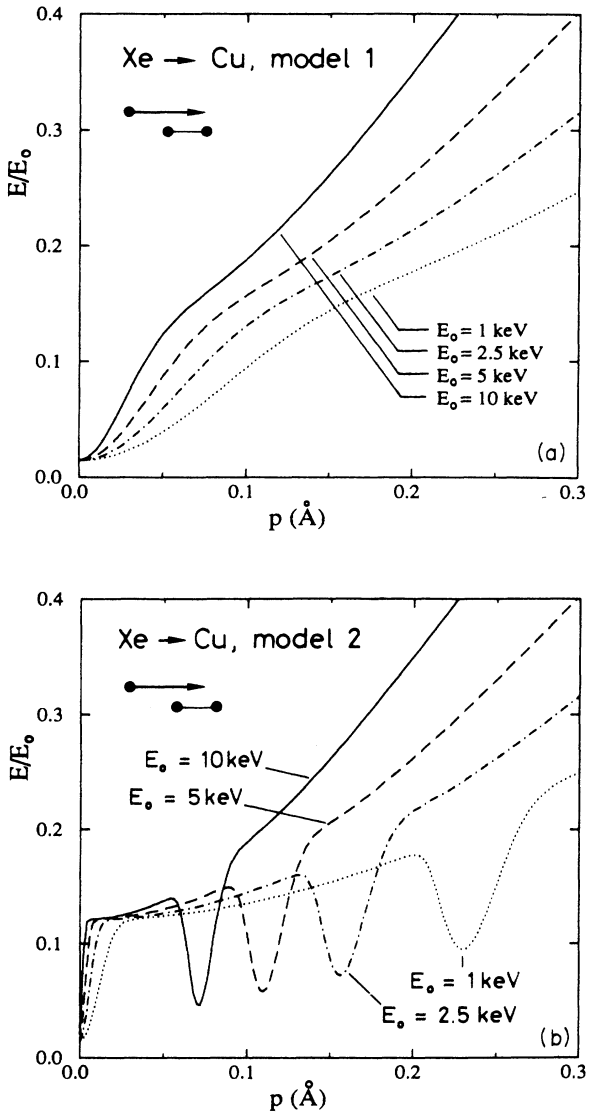

FIG. 5. Same collision as in Fig. 2 with varying initial energy E_0. We plot the ratio between final and initial energy E/E_0. (a) Model 1. (b) Model 2.

range of impact parameters where nonlinearities show up.

So far, all results refer to dimers oriented parallel to the initial direction of motion. Figures 7(a)-7(c) show results for a dimer inclined at an angle $\psi = 10°$ with the projectile velocity. Impact parameters lie in a plane defined by the dimer axis and the velocity, i.e., all motion is still restricted to a plane, and $p = 0$ refers to a central collision with atom 1. Unlike in the previous figures, there is no reflection symmetry around $p = 0$. Apart from minor quantitative differences between model 1 and model 2, a major difference is found in the E versus θ dependence for $-20° \leq \theta \leq 0°$.

In order to illustrate what is going on, pertinent trajectories are shown in Figs. 8(a)-8(f). Figures 8(a) and 8(b) show that the nonlinearities observed in Figs. 7(a) and 7(b) at $p = -0.18$ Å are due to atom 2 approaching the ion trajectory at the right time. Figures 8(c) and 8(d) show a similar effect at $p = -0.08$ Å, although here it is atom 1, after scattering on atom 2, that undergoes a second interaction with the ion and causes spikes in Figs. 7(a) and 7(b). Finally, Figs. 8(e) and 8(f) demonstrate a very pronounced effect of a very subtle cause: the very slow motion of atom 2 initiated by atom 1.

Figures 9(a) and 9(b) show a case of nonplanar motion where the impact point of the ion lies outside the plane defined by the initial velocity of the ion and the dimer axis. It is seen that in this situation only one case of nonlinearity, the clearing-the-way effect, remains: The energy loss is decreased for $p < 0.1$ Å just as in Fig. 2(a). The opposite effect, blocking the trajectory at the right time, resulting in an increased energy loss in Fig. 2(a) for 0.1 Å $< p < 0.14$ Å, has been effectively eliminated. This feature must be expected to be more general: Scattering in and out of a trajectory may well be equally likely events in two dimensions, while in three dimensions,

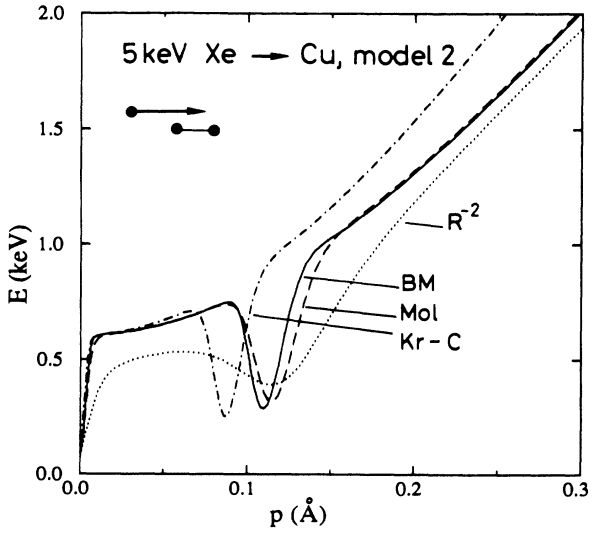

FIG. 6. Same collision as in Fig. 2 but for different ion-atom and atom-atom potentials. BM: Born-Mayer potential, lower case in Eq. (1); Mol: Moliere potential with Lindhard screening radius; Kr-C (Ref. 6); R^{-2} = upper case in Eq. (1).

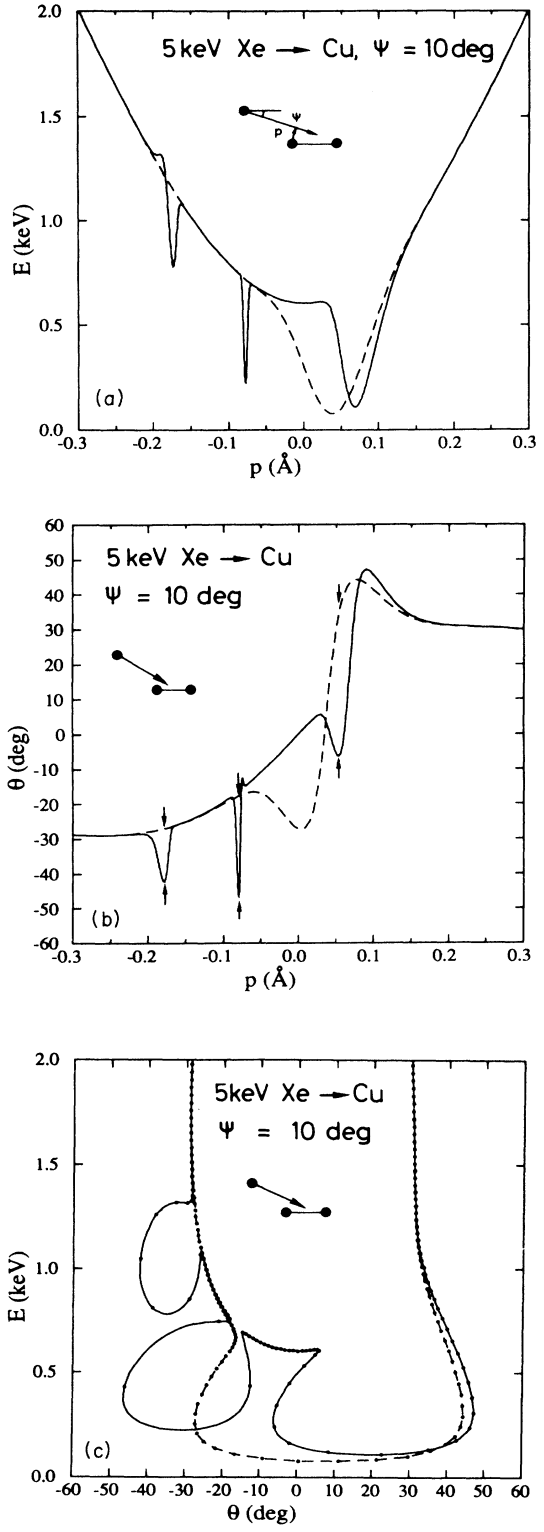

FIG. 7. Same collision as in Fig. 2 but with dimer axis inclined $\psi = 10°$ against projectile velocity. Impact parameter scanned within the plane made up by the dimer and the projectile velocity. (a) Energy vs impact parameter. (b) Scattering angle vs impact parameter. Arrows indicate impact parameters for which trajectories are shown in Fig. 8. (c) Energy vs scattering angle. Dots as in Fig. 2(c).

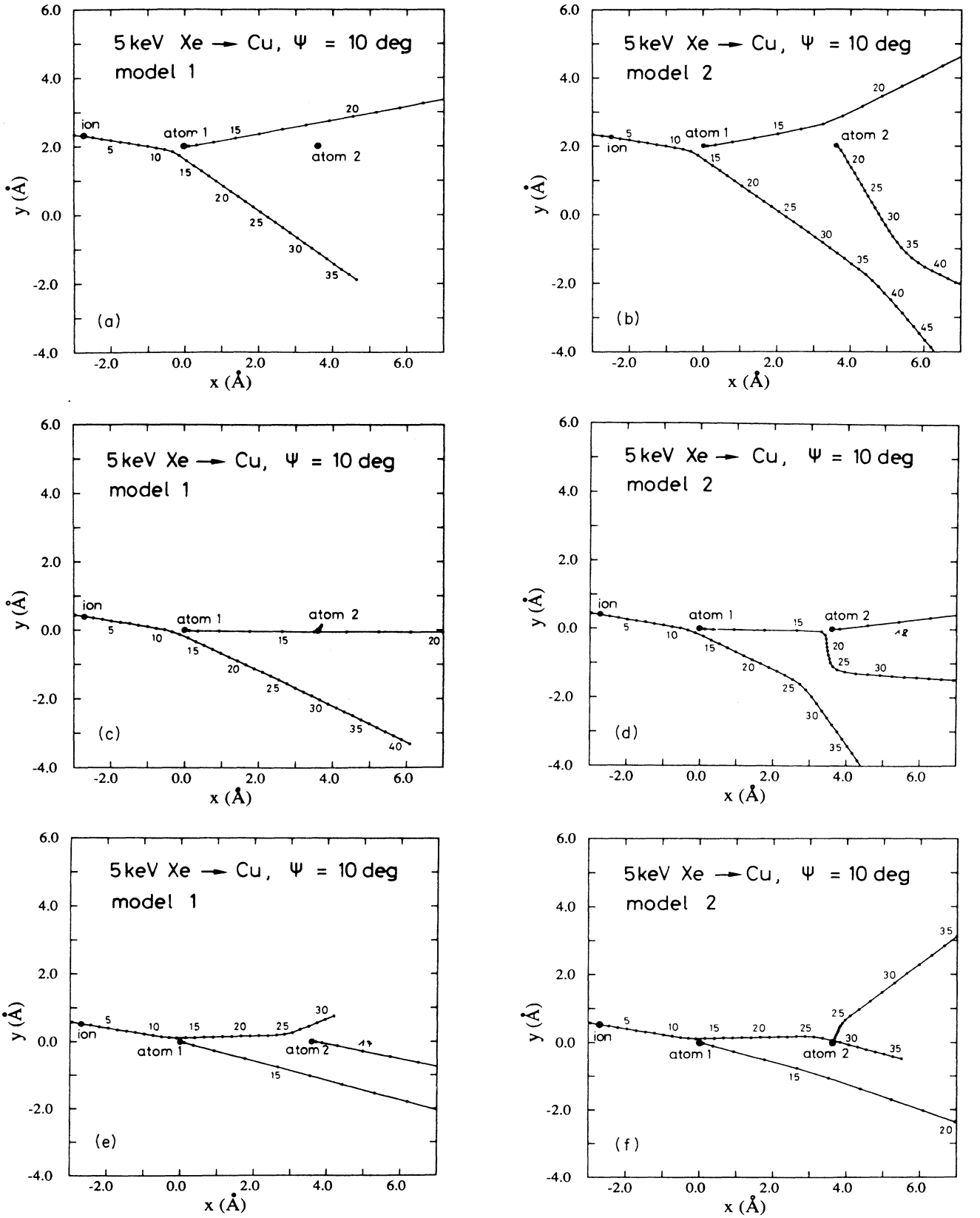

FIG. 8. Trajectories for collisions specified in Fig. 7 for specific impact parameters. Planar motion. (a) $p = -0.18$ Å. Model 1. (b) $p = -0.18$ Å. Model 2. (c) $p = -0.08$ Å. Model 1. (d) $p = -0.08$ Å. Model 2. (e) $p = 0.053$ Å. Model 1. (f) $p = 0.053$ Å. Model 2.

availability of space makes scattering out more likely than scattering in.

Figure 10 shows plots of energy versus scattering angle for a series of inclination angles in the case of planar motion similar to Fig. 7(c). When the inclination angle ψ exceeds 10° a loop forms with a position at $\theta \cong 2\psi$, i.e., at specular reflection. Moreover, a spike toward low scattering angles at high energy loss develops for even larger inclination angles: This indicates the opening up of hard collisions with atom 2 and hence, the possibility of the ion breaking through the dimer.

Figures 11(a) and 11(b) show energy versus scattering angle for a randomly oriented dimer. The density of points reflects the intensity in a collision experiment on randomly oriented copper molecules to the extent that the ion-target and target-target potential (1) is valid. The two graphs, being constructed on the basis of model 1 [Fig. 11(a)] and model 2 [Fig. 11(b)], look completely identical, although a point-by-point comparison (not documented here) reveals that they are only very similar. Evidently, the dominating fraction of the solid angle is occupied by dimer orientations where the interaction between the two recoiling target atoms does not noticeably affect the outcome of the collision event.

This is different when the orientation is averaged only over a limited fraction of the solid angle. Figures 11(c) and 11(d) show such data for $0 \leq \psi \leq 10°$. A strikingly nonlinear behavior is found in the lower half of the figure, i.e., for low exit energy or high energy loss. As was to be expected from Fig. 2, the binary collision portion is well developed in the nonlinear case [Fig. 11(b)] but almost absent in the linear case [Fig. 11(a)], as far as the low-E portion is concerned.

We conclude that measurable nonlinear behavior must stem exclusively from small inclination angles ψ.

Figure 12(a) shows the scattering on a linear chain inclined at an angle $\psi = 18°$ which can be compared to that on a corresponding dimer [Fig. 10]. The most prominent difference is seen to be the absence of a hard, binary collision portion in case of the linear chain. Instead, a closed loop is formed. Loops of simpler shape are well established in ion scattering from surfaces for $M_1 < M_2$.[14,15] In Fig. 12(b), an extra row of atoms has been added underneath the linear chain. While this row does not affect the scattering distribution in the regime of nearly specular deflection (the upper loop), evidence for nonlinear effects is found in the lower part. Although the calculated excursions from linear behavior seem dramat-

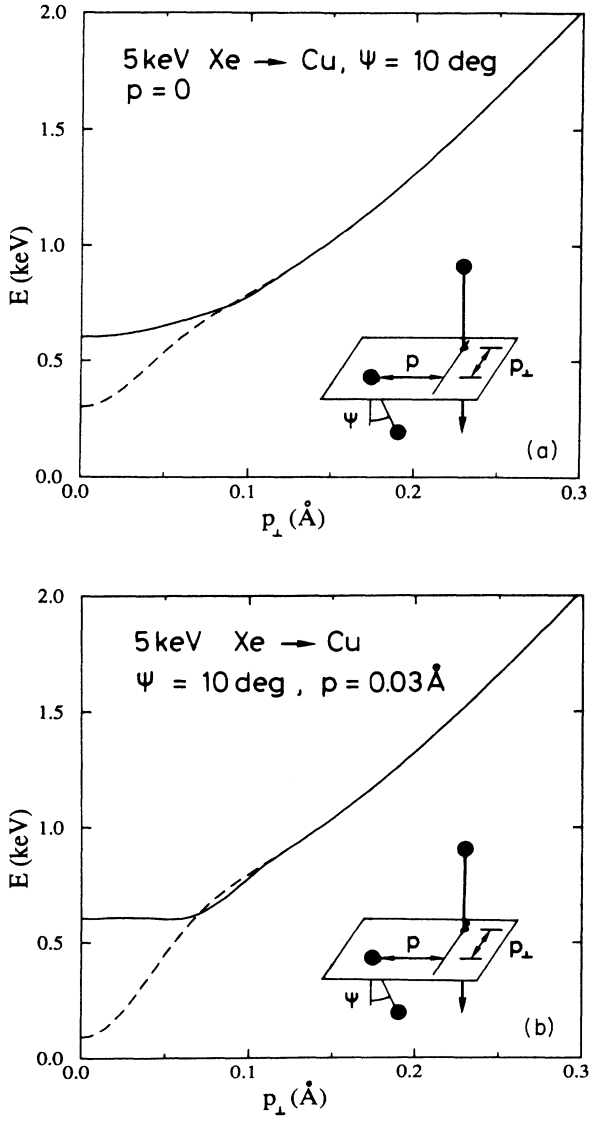

FIG. 9. Same collision as in Fig. 2 with the dimer axis inclined $\psi = 10°$ against the projectile velocity. Impact parameter scanned perpendicular to the plane made up by the dimer and the projectile velocity. (a) Parallel position corresponding to $p = 0$ in Fig. 7. (b) Parallel position corresponding to $p = 0.03$ Å in Fig. 7.

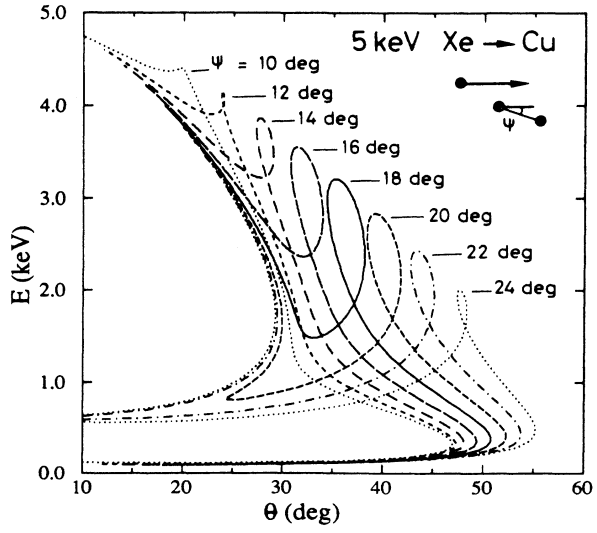

FIG. 10. Same collision as in Fig. 2 for a series of inclination angles ψ. Planar motion. Model 2 only. The inner envelope is the binary collision limit.

ic, the density of points is very low, indicating that in an experiment, predicted effects may overshadowed by noise.

Figure 13 shows representative trajectories corresponding to the collision geometry shown in Fig. 12(a), i.e., the collision with an isolated chain of five atoms. In Fig. 13(a) the ion hits slightly to the right of atom 3, and in Figs. 13(b)–13(e) it aims increasingly toward the left, but always toward the right of atom 2. It is evident that at no impact parameter does the ion break through the chain. This explains why there are no nonlinearities: Figs. 8(b) and 8(d) demonstrate that nonlinear behavior requires the ion to hit a target atom "from the left" in the geometry chosen. The perfect string does not allow this at an angle of 18°. This would be different in the presence of steps, surface vacancies, or small overlayers of dimers, trimers, etc.

Inspection of Figs. 13(a)–13(e) reveals that the maximum scattering angle shown in Fig. 12(a) corresponds to the trajectory shown in Fig. 13(d), while the crossing point in Fig. 12(a) corresponds to the trajectories shown in Figs. 13(c) and 13(e). A detailed discussion of the nonlinearities found in Fig. 12(b) on the basis of the corresponding trajectories will be reserved for a later investigation.

IV. IMPLICATIONS

A. Stopping cross section

Our initial motivation for this study was an expectation[1] that the stopping power of a heavy ion due to elastic

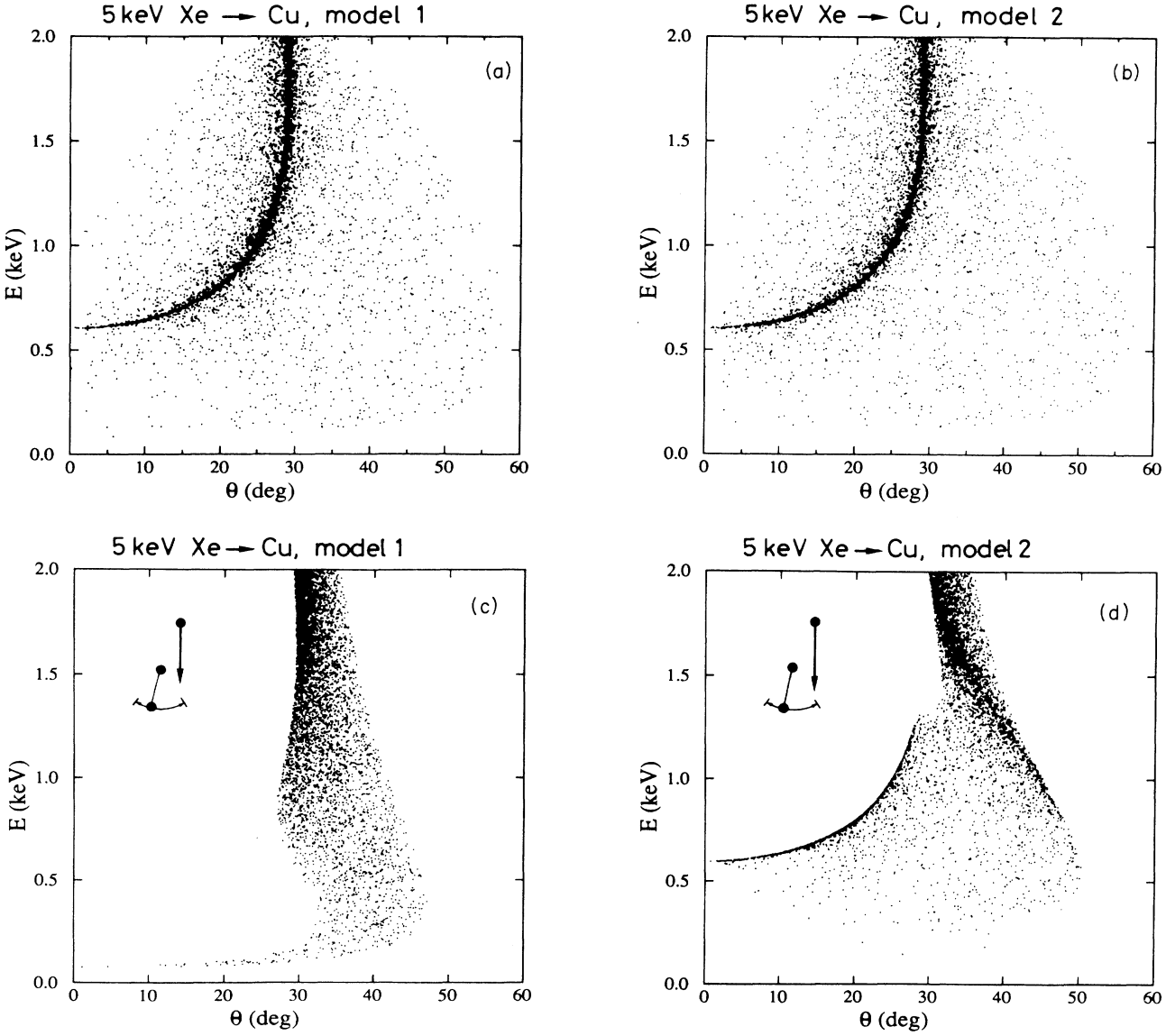

FIG. 11. Same collision as in Fig. 2 for $d = 2.22$ Å, i.e., the internuclear distance of a Cu_2 molecule randomly oriented. (a) Model 1. (b) Model 2. (c) Average over $0 \leq \psi \leq 10°$ only; model 1. (d) Same as (c); model 2.

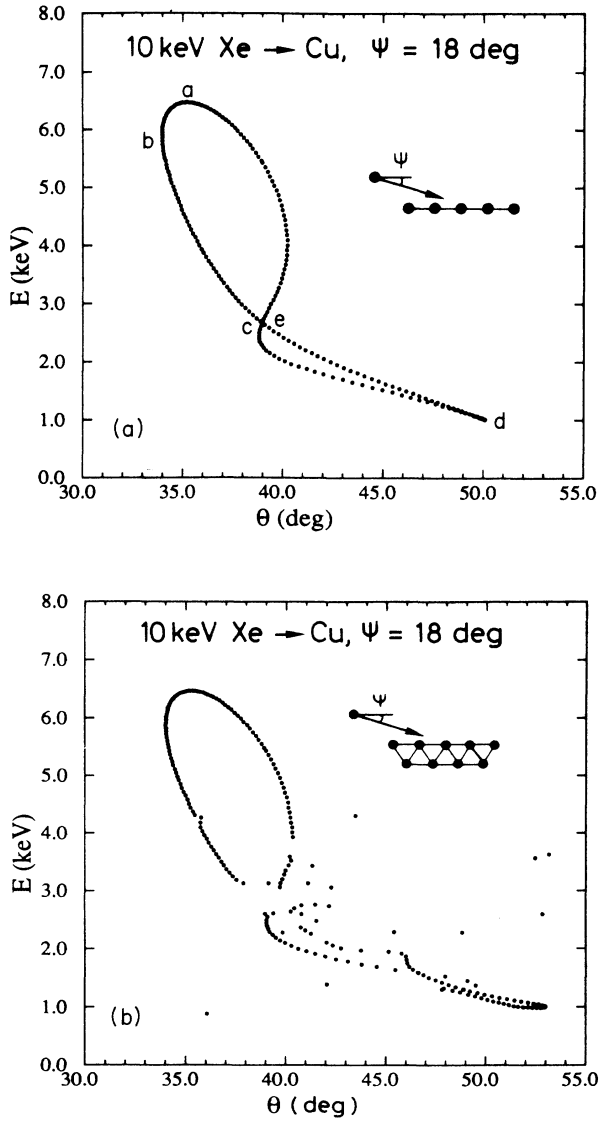

FIG. 12. Scattering on linear chain. 10-keV Xe on Cu. $\psi = 18°$. Planar motion. (a) Linear chain containing five atoms. The impact parameter was scanned between the midpoints of atoms 2 and 3, and atoms 3 and 4, respectively, in order to avoid edge effects due to the finite length of the chain. (b) Same as (a) with an additional atom layer underneath.

collisions might be affected by nonlinear effects of the type described here.

Figure 9 presents clear evidence that fast recoils may clear the way for the projectile and thus give rise to a decrease in stopping power via a decrease in effective atomic density in the vicinity of the ion track. Since only dimer targets have been considered so far, a conclusive estimate of the magnitude of this nonlinear effect in a dense solid cannot yet be given. However, since the effect hinges on rather close collisions—which are infrequent—it will hardly affect the stopping power drastically.

For a qualitative estimate, consider the dimer, Figs. 9(a) and 9(b). Approximate the difference in energy between model 1 and model 2 by a constant value of 0.5 keV in the interval $0 \leq p \leq 0.1$ Å. This (rather generous) estimate results in a difference in stopping cross section of about 15 eV Å^2. This value could be compared with the stopping cross section of a copper atom for 5-keV xenon [found from conventional stopping theory or by extrapolation of Fig. 2(a)] which is of the order of 10 keV Å^2. Thus, for dimers, the stopping cross sections predicted from models 1 and 2 differ from each other by about 0.1%.

B. Ion-molecule collisions under single scattering conditions

A scaling law has been derived previously,[8] relating a characteristic (e.g., a most probable) energy loss T_0 to the scattering angle in electronically elastic ion-molecule collisions under single-scattering conditions,

$$T_0 = (M_1/M_2) E_0 \theta^2 f(E_0 \theta) , \tag{2}$$

for a homonuclear diatomic molecule, where f is a function depending on the ion-atom potential.

Equation (2) has been derived by means of the scaling laws of classical perturbation theory, i.e., for soft collisions. Experimental tests[16,17] were performed in part on systems where $M_1 > M_2$, e.g., on hydrogen targets bombarded by heavier ions.

The question arises to what extent the scaling law (2) is affected by nonlinear effects. It is seen from Figs. 11(a) and 11(b) that for randomly oriented molecules, the linear and nonlinear model make essentially identical predictions for the distribution in energy loss versus scattering angle. For a partially oriented collection of molecules, this is not so. Although the two models make similar predictions for $E = 5$ and 1.5 keV, i.e., for the region where the single scattering law predicts the energy loss to *increase* for *increasing* scattering angle, a drastically different behavior is observed for $E < 1.5$ keV, where model 2 predicts a high statistical weight for single scattering behavior which would be identified as "spectator collisions" in the absence of nonlinear behavior.

For $M_1 > M_2$, the energy distribution of scattered ions at a given scattering angle must in principle show at least two peaks which may in practice be more or less separable for a randomly oriented molecule. The scaling law (2) can, from the outset, only be expected to be valid for the low-loss, or high-energy peak, since perturbation theory cannot be valid for the high-loss peak. The present work adds the fact that the high-loss peak, in addition to not obeying perturbation theory, is also affected by nonlinearity which, of course, was not considered in the derivation[8] of Eq. (2).

We conclude that the present results do not affect the validity of the scaling law (2) as discussed in Refs. 8 and 17. It is, however, evident that Eq. (2) cannot be expected to hold if T_0 were taken to be the *average energy loss* rather than the appropriate *peak energy loss* at a given scattering angle, since the average includes a range of energies where Eq. (2) does not apply.

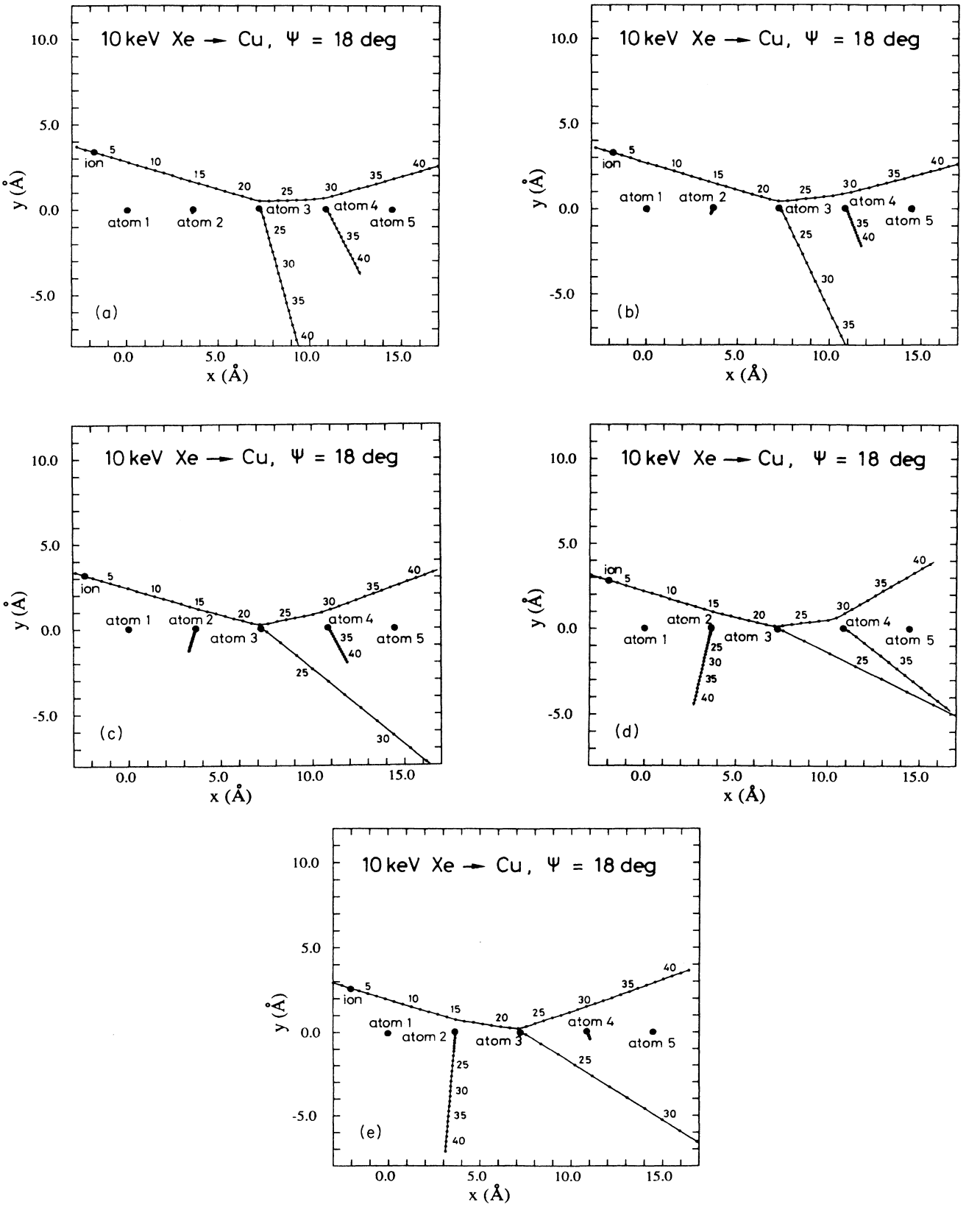

FIG. 13. Trajectories for collision on an isolated chain of five atoms. To be compared with Fig. 8. Model 2 only. Impact parameters relative to the center atom (atom 3) of the chain. (a) $p = 0.426$ Å. (b) $p = 0.316$ Å. (c) $p = 0.062$ Å. (d) $p = -0.164$ Å. (e) $p = -0.383$ Å.

C. Ion-surface scattering

Ion-surface scattering experiments at keV and eV energies are most often performed under conditions where $M_1 < M_2$. The most obvious reasons for this are as follows: (i) Binary collision kinematics is comparatively simple, implying a unique relation between energy loss and scattering angle of the projectile, (ii) there are always backscattered ions, regardless of the angle of incidence, and (iii) there is a well-defined shadow cone behind each surface atom in a binary collision.

A most important result of the present work is the observation of a pronounced backscattering loop from a linear chain even for $M_1 > M_2$ (Fig. 12), not unlike those observed for light ions.[14,15,18]

In the region of nearly specular reflection, i.e., the upper loop in Fig. 12(a), there does not seem to be evidence for nonlinear behavior. This may be an important simplifying aspect if heavier ions ($M_1 > M_2$) are to be used as a tool in ion scattering spectroscopy.

Nonlinear effects do influence the overall behavior at large (nonspecular) scattering angles but their statistical weight appears surprisingly small under the conditions investigated here.

Pronounced single scattering behavior in the high-loss portion of the energy versus angle diagram may be taken as evidence for the presence of dimers or steps on a surface. This feature is specific to ion-surface scattering under conditions where $M_1 > M_2$. The latter aspect, as well as a more detailed investigation of ion-surface scattering involving more comprehensive data on polyatomic targets will be reserved to later work.

V. SUMMARY

(1) When the projectile mass M_1 exceeds the mass of a target atom M_2, recoil atoms may move noticeably faster than the projectile. Therefore, recoil atoms may modify the spatial configuration of the target in front of the ion before the arrival of the latter.

(2) This effect, which is insignificant for the light projectiles interacting with heavy target atoms, is to be regarded as nonlinear, since it invokes a feedback of changes, brought about in the target by the projectile, on that same projectile.

(3) Recoil atoms may clear as well as block the way for the projectile. For motion in a plane, clearing and blocking action are observed each in their respective domains of impact parameter, and are about equally pronounced. For three-dimensional motion, clearing the way appears to be dominating. Therefore, scattering events become less frequent because of a decrease in effective target density seen by the projectile.

(4) The cases analyzed so far are all based on very few, most often two, target atoms. For dimer targets, the most pronounced feature is a wider range of impact parameters where collisions are effectively binary, than what one would expect from linear superposition of two binary events.

(5) In the field of ion-molecule collisions, events obeying binary-collision kinematics are commonly interpreted as "spectator" collisions where one target atom is more or less unaffected in a collision. We find that for $M_1 > M_2$, such an observed binary-collision character may also be evidence of the opposite behavior, i.e., a nonlinear effect where, on the contrary, one target atom which would otherwise be hit by the ion is actually kicked out of its way before arrival.

(6) For $M_1 > M_2$, ion-molecule scattering is affected by nonlinear effects mainly in the regime of increasing energy loss with *decreasing* scattering angle, i.e., for hard collisions. This is one more reason for the fact that a simple scaling law for ion-molecule collisions, derived by one of us,[8] can only be valid in the regime of soft collisions, i.e., for the low-loss peak in the energy spectrum of scattered ions at any scattering angle. The other reason (evident from the outset) is the use of perturbation theory in the derivation. For both reasons, the scaling law should not be utilized for an average energy loss.

(7) Because of the restriction to dimer targets, no conclusive statement has yet been made on the effect of nonlinearity on stopping power. For dimers oriented along the beam, the effect is found to be exceedingly small because of compensation. For randomly oriented dimers, a decrease in the stopping cross section of the order of 0.1% has been found.

(8) Ion-surface scattering has been modeled by a chain of five atoms. A closed loop is found, not unlike those found for $M_1 < M_2$ in the energy versus angle diagram. It has the shape of a deformed figure eight. Nonlinear effects are observed in the lower part only when an extra row of atoms is inserted underneath. These nonlinearities are not very pronounced.

(9) A specific feature of ion-surface scattering under conditions where $M_1 > M_2$ is the possibility of identifying steps and dimers on the basis of pronounced binary-scattering events, by nonlinear behavior.

ACKNOWLEDGMENTS

This work was supported by the Danish Natural Science Research Council (V.I.S) and the Danish Research Academy (M.V.).

---

*Permanent address: Institute of Nuclear Physics, Moscow State University, Moscow 119 899 U.S.S.R.

†Present address: Institut für Theoretische Physik, Technische Universität, D-33 Braunschweig, Federal Republic of Germany.

[1] P. Sigmund, lecture delivered at the NATO Advanced Study Institute, Viana do Castelo, Portugal, 1987 (copies available from the author).

[2]J. A. Brinkman, J. Appl. Phys. **25**, 961 (1954).
[3]P. Sigmund, Appl. Phys. Lett. **25**, 169 (1974); **27**, 52 (1975).
[4]G. Carter, Radiat. Eff. Lett. **43**, 193 (1979); **50**, 105 (1980).
[5]P. Sigmund, Rev. Roum. Phys. **17**, 823 (1972); **17**, 969 (1972); **17**, 1079 (1972).
[6]J. P. Biersack and L. Haggmark, Nucl. Instrum. Methods **174**, 257 (1980).
[7]M. T. Robinson and I. M. Torrens, Phys. Rev. B **9**, 5008 (1974).
[8]P. Sigmund, J. Phys. B **11**, L145 (1978).
[9]D. E. Harrison, Radiat. Eff. **70**, 1 (1983).
[10]V. I. Shulga, Radiat. Eff. **51**, 1 (1980).
[11]D. E. Harrison, W. L. Gay, and H. M. Effron, J. Math. Phys. **10**, 1179 (1964).
[12]J. B. Gibson, A. N. Goland, M. Milgram, and G. H. Vineyard, Phys. Rev. **120**, 1229 (1960).
[13]O. B. Firsov, Zh. Eksp. Teor. Fiz. **33**, 696 (1957) [Sov. Phys.—JETP **6**, 534 (1957)].
[14]V. M. Kivilis, E. S. Parilis, and N. Yu. Turaev, Dokl. Akad. Nauk SSSR **173**, 805 (1967) [Sov. Phys. Dokl. **12**, 328 (1967)].
[15]V. E. Yurasova, V. I. Shulga, and D. S. Karpuzov, Can. J. Phys. **46**, 759 (1968).
[16]N. Andersen, M. Vedder, A. Russek, and E. Pollack, Phys. Rev. A **21**, 782 (1980).
[17]M. Vedder, H. Hayden, and E. Pollack, Phys. Rev. A **23**, 2933 (1981).
[18]W. Heiland, E. Taglauer, and M. T. Robinson, Nucl. Instrum. Methods **132**, 655 (1976).